

Supporting information for High-Performance Aqueous Supercapacitors Based on Hierarchically Porous Graphitized Carbon

Zheng Chen,^a Ding Weng,^a Hiesang Sohn,^a Mei Cai,^{*b} and Yunfeng Lu^{*a}

^a Department of Chemical and Biomolecular Engineering, University of California, Los Angeles, CA 90095, Fax: 310-206-410; Tel: 310-794-7238; E-mail: luucla@ucla.edu; ^b General Motor R&D Center, Warren, MI 48090, USA, E-mail: mei.cai@gm.com

Synthesis of hierarchically porous graphitized carbon particles: In a typical synthesis, aqueous solutions containing 40 mL of de-ionized water, 12 g of sucrose, 10 g of nickel nitrate, 20 g of 0.1 M HCl and silicate templates (20 g of colloidal silica particles (AS 30%, Nissan Chemicals. Inc.) and 16 g of TEOS) were sent through an atomizer using nitrogen as carrier gas. The atomizer dispersed the solution into aerosol droplets, which were then passed through a ceramic tube that was heated to 450 °C. Continuous solvent evaporation at the air/liquid interface of the aerosol droplets enriched the sucrose and silica, resulting in the formation of spherical silica/sucrose/nickel moiety nanocomposite particles. The particles were then collected on a membrane filter in a press, and subsequent carbonization to 900 °C of the composite nanoparticles under N₂ atmosphere resulted in the formation of spherical silica/carbon/nickel composite nanoparticles. 1 M HCl and 5 M NaOH were used in sequence to remove the nickel and silica respectively, which produced the porous carbon particles with graphitized shell structure.

Material characterization: The X-ray diffraction measurements were taken on Panalytical X'Pert Pro X-ray powder diffractometer using the copper K α radiation ($\lambda=1.54$ Å). Nitrogen sorption isotherms were measured at 77K with a Micromeritics ASAP 2020 analyzer. All the samples were degassed in vacuum at 180°C for three hours. The specific surface areas (S_{BET}) were calculated by the Brunauer-Emmett-Teller (BET) method using adsorption branch in a relative pressure range from 0.04 to 0.25. The pore size distributions (D_p) were derived from the adsorption branches of isotherms

using the Barrett-Joyner-Halenda (BJH) model. Scanning electron microscopy (SEM) experiments were conducted on a JEOL JSM-6700 FE-SEM. Transmission electron microscopy (TEM) experiments were conducted on a Philips CM120 operated at 120 kV. The Raman spectrum was recorded by a Jobin Yvon micro-Raman spectroscope (Super LabRam II) with a mode of 50×objective (8 mm), a holographic grating (1800 g mm⁻¹), 1024 × 256 pixels charge-coupled device detector and 5 mW He-Ne laser at 632.8 nm as an excitation line. Each Raman spectrum was obtained using three accumulations, and the acquisition time in each case was typically 8 s.

Electrochemical test: All the electrodes were prepared by a slurry-coating process using nickel foam as substrates. Briefly, 80% of the testing materials, 10% carbon black, and 10% poly(vinylidene fluoride) (PVDF) dispersed in N-methylpyrrolidinone (NMP) were mixed to form slurries. The slurries were ultrasonically treated at 60°C for 0.5 h, coated on a nickel foam substrates, and dried at 80°C for 10 min under vacuum. As formed electrodes were then pressed at a pressure of 2 M Pa and further dried under vacuum at 100°C for 12 h. The electrochemical measurements were conducted in a Solartron 1287 electrochemistry workstation. The specific capacitance (C) of the electrode materials were derived from $C = I/(dE/dt) \approx I/(\Delta E/\Delta t)$, where I is the constant discharge current density, E is cell voltage, and dE/dt is slope of the discharge curve.

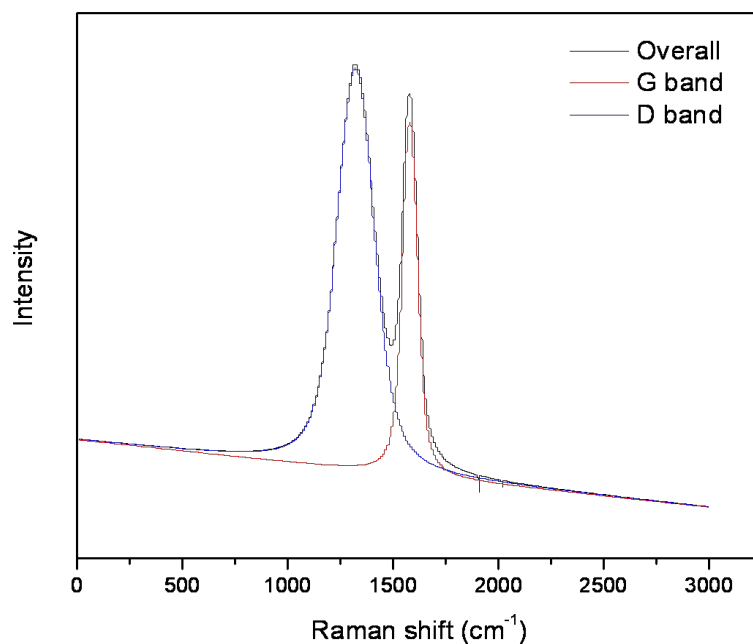


Fig. S1. Raman spectrum of the porous graphitized carbon particles.

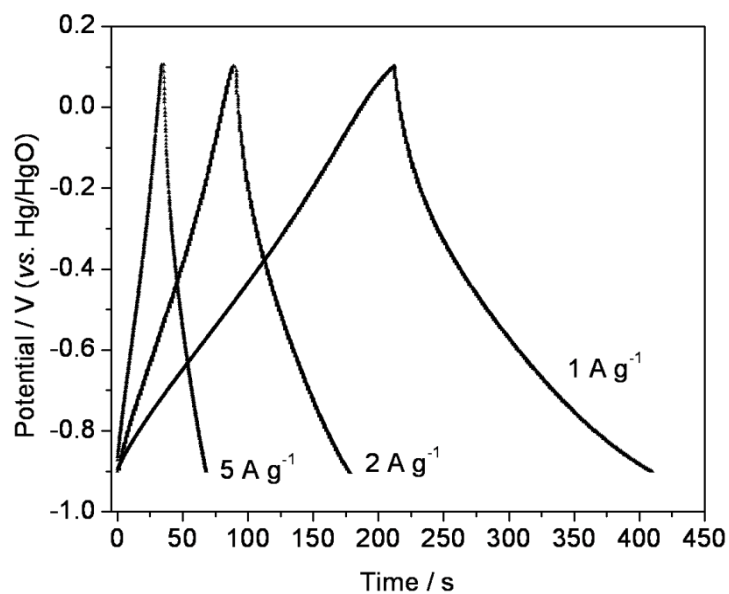


Fig. S2. Galvanostatic charge/discharge curves of porous graphitized carbon electrodes at different current densities in 3 M KOH aqueous electrolyte.

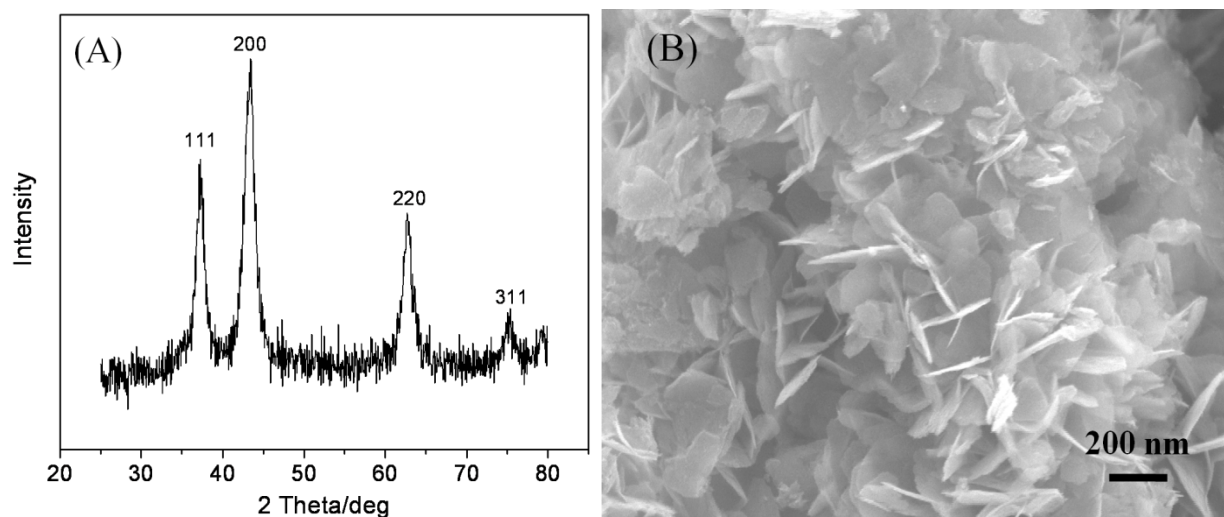


Fig. S3. XRD pattern (A) and SEM image (B) of NiO nano-flakes.

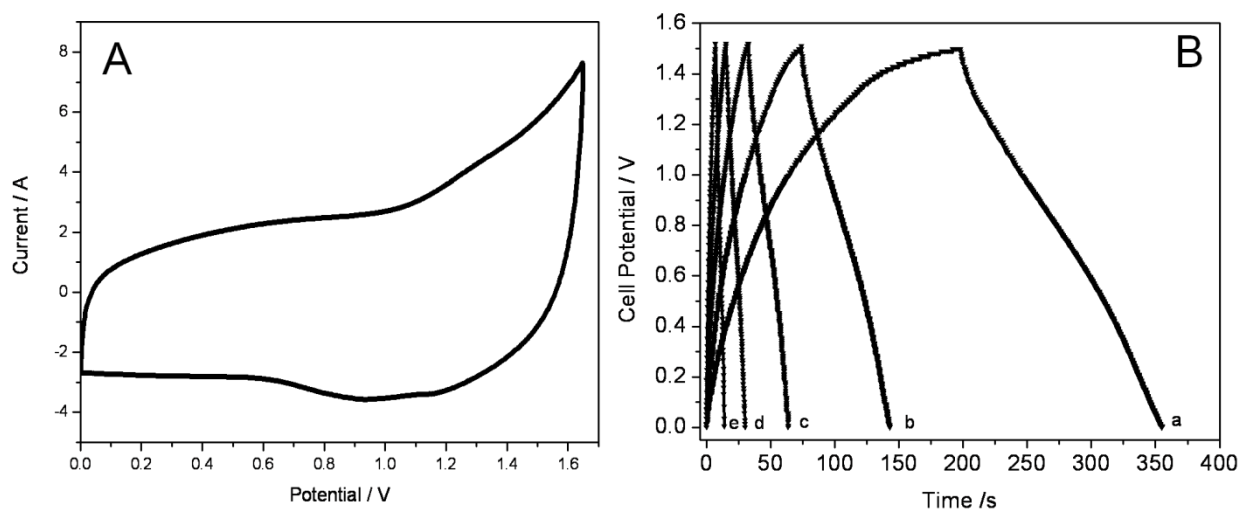


Fig. S4. CV of a prototype asymmetric carbon/NiO device at 2 mV s^{-1} using porous carbon particles as anode and NiO as cathode (A); and galvanostatic charge-discharge curves at various current density (a: 1.5 mA cm^{-2} ; b: 3.1 mA cm^{-2} ; c: 6.2 mA cm^{-2} ; d: 12.5 mA cm^{-2} ; e: 24.6 mA cm^{-2}) of NiO-aerosol carbon in 3 M KOH (B).

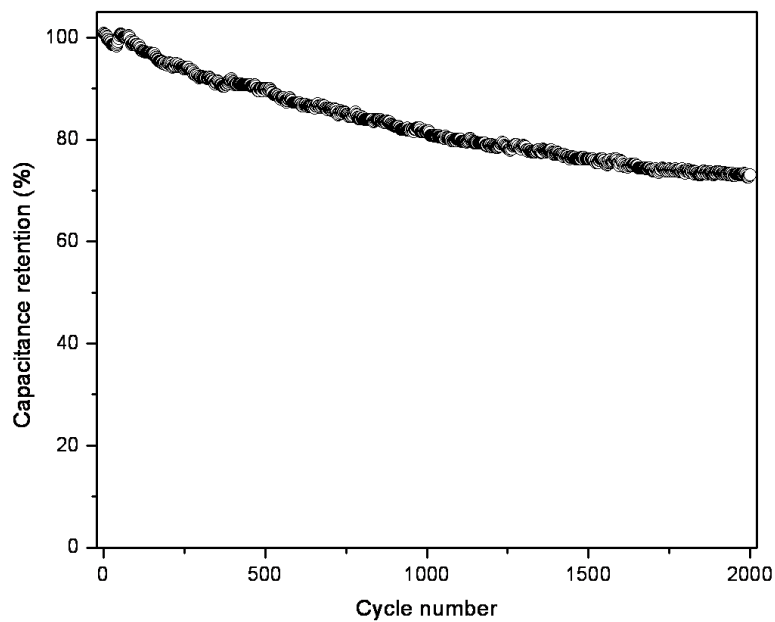


Fig. S5. Cycling performance of the Carbon/NiO asymmetric capacitor.

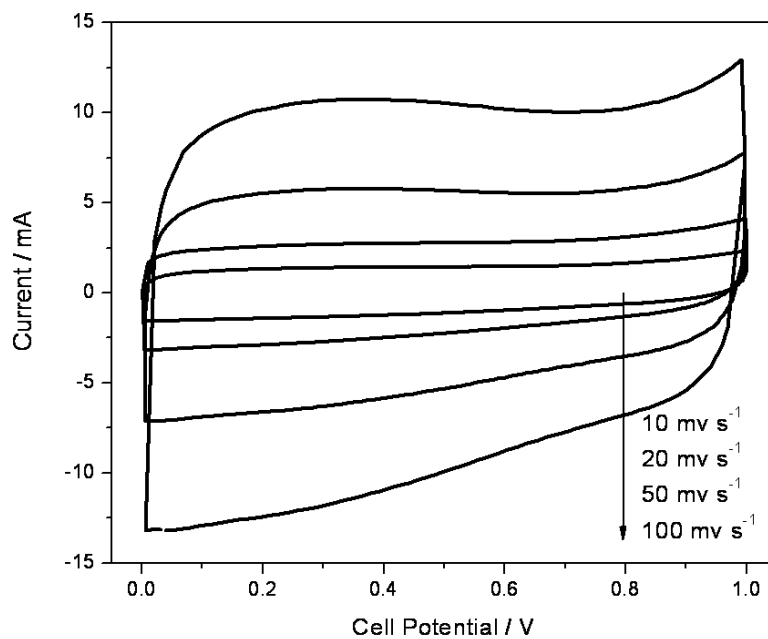


Fig. S6. CVs of symmetric supercapacitor with porous carbon particle electrodes.

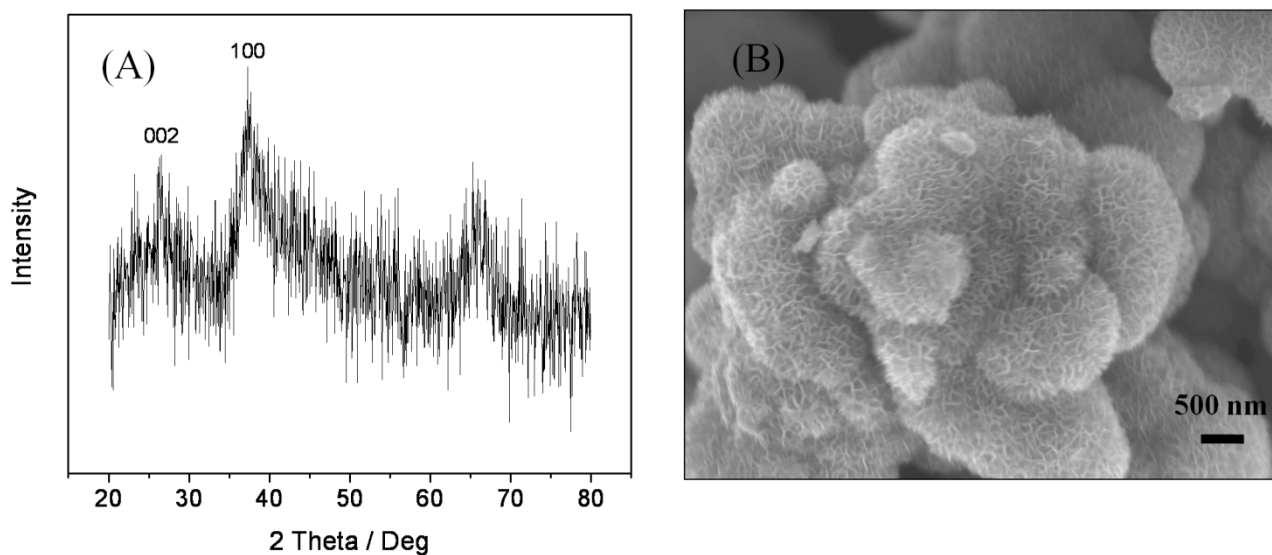


Fig. S7. XRD pattern (A) and SEM image (B) of MnO₂/C nanocomposite for asymmetric carbon/MnO₂ devices.

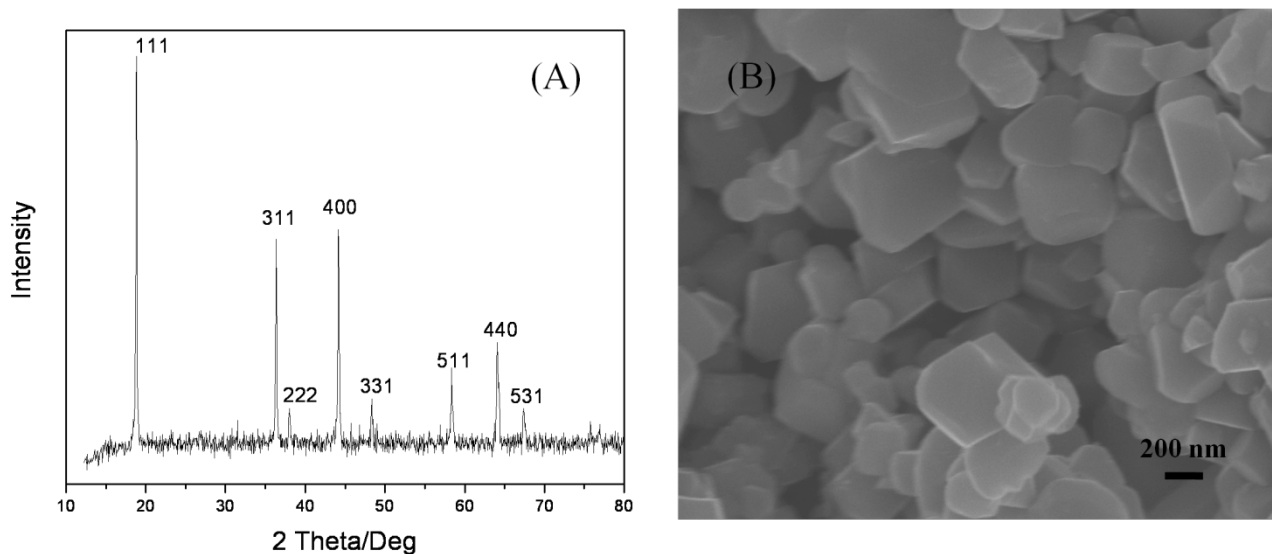


Fig. S8. XRD pattern (A) and SEM image (B) of LiMn₂O₄ nanoparticles for asymmetric carbon/LiMn₂O₄ devices.